



## A new supramolecular cocrystal of 2-amino-3-bromopyridine with 4-methylbenzoic acid: Synthesis, structural, spectroscopic characterization and comparative theoretical studies

Kaliyaperumal Thanigaimani, Nuridayanti Che Khalib, Suhana Arshad, Ibrahim Abdul Razak & Madhukar Hemamalini

**To cite this article:** Kaliyaperumal Thanigaimani, Nuridayanti Che Khalib, Suhana Arshad, Ibrahim Abdul Razak & Madhukar Hemamalini (2016) A new supramolecular cocrystal of 2-amino-3-bromopyridine with 4-methylbenzoic acid: Synthesis, structural, spectroscopic characterization and comparative theoretical studies, *Molecular Crystals and Liquid Crystals*, 625:1, 259-275, DOI: [10.1080/15421406.2015.1081031](https://doi.org/10.1080/15421406.2015.1081031)

**To link to this article:** <http://dx.doi.org/10.1080/15421406.2015.1081031>



Published online: 19 Feb 2016.



Submit your article to this journal [↗](#)



Article views: 76



View related articles [↗](#)



View Crossmark data [↗](#)

# A new supramolecular cocrystal of 2-amino-3-bromopyridine with 4-methylbenzoic acid: Synthesis, structural, spectroscopic characterization and comparative theoretical studies

Kaliyaperumal Thanigaimani<sup>a</sup>, Nuridayanti Che Khalib<sup>a</sup>, Suhana Arshad<sup>a</sup>, Ibrahim Abdul Razak<sup>a</sup>, and Madhukar Hemamalini<sup>b</sup>

<sup>a</sup>X-ray Crystallography Unit, School of Physics, Universiti Sains Malaysia, Penang, Malaysia; <sup>b</sup>Department of Chemistry, Vel Tech Multi Tech, Avadi, Chennai, Tamil Nadu, India

## ABSTRACT

The 1:1 cocrystal of 2-amino-3-bromopyridine (2A3BP) with 4-methylbenzoic acid (4MBA) has been prepared by slow evaporation method in methanol, which was crystallized in monoclinic  $P2_1/c$  space group having two molecules in the asymmetric unit. The cocrystal has been characterized by single crystal X-ray analysis, FTIR,  $^1\text{H}$  NMR,  $^{13}\text{C}$  NMR, and Powder XRD. Theoretical investigations have been calculated by HF and density function (B3LYP) method with the 6-311+G(d,p) basis set. The vibrational frequencies together with the  $^1\text{H}$  NMR and  $^{13}\text{C}$  NMR chemical shifts have been calculated on the fully optimized geometry of **1**. Theoretical calculations of bond parameters, harmonic vibration frequencies, and isotropic chemical shifts are in good agreement with the experimental results. Solvent-free formation of these cocrystal was confirmed by powder X-ray diffraction analysis. The crystal structure was stabilized by  $\text{N}_{\text{pyridine}}\cdots\text{O}=\text{C}$ ,  $\text{C}=\text{O}\cdots\text{H}\cdots\text{N}_{\text{pyridine}}$  and  $\text{C}\cdots\text{Br}$  hydrogen bonding interactions.



## KEYWORDS

Cocrystal; DFT calculations; FTIR and NMR Spectroscopy; Hartree-Fock; 2-amino-3-bromopyridine; 4-methylbenzoic acid

## Introduction

Cocrystals, one of the synthetic targets in crystal engineering, are a long known class of compounds, but they were not extensively studied until the late 1990s when they became recognized as valuable materials [1–5]. Even now, more than one hundred years after the first cocrystals were reported [6, 7] the definition of the term cocrystal is a topic for discussion [8–10]. By cocrystallization, a crystalline complex of two or more molecules is constituted, bonding together in the crystal lattice through non-covalent interactions such as hydrogen bonding [11]. The technique of cocrystallization continues to gain significance for its application to the design of new supramolecular structures with desired functional properties [12–15]. Most recently, in the field of pharmaceuticals, cocrystallization has been shown to be an effective means of altering a drug's physical properties, such as stability, solubility, and melting point [16–19].

Pyridine derivatives are one of the most used frameworks for medicines, food flavorings, dyes, agrochemicals, rubber chemicals, and adhesives [20]. In drug discovery, it was

**CONTACT** Ibrahim Abdul Razak  [arazaki@usm.my](mailto:arazaki@usm.my)  Assoc. Professor of Physics, X-ray Crystallography Unit, School of Physics, Universiti Sains Malaysia, 11800 USM, Penang, Malaysia.

Color versions of one or more of the figures in the article can be found online at [www.tandfonline.com/gmcl](http://www.tandfonline.com/gmcl).

© 2016 Taylor & Francis Group, LLC

well demonstrated that to avoid screening millions of compounds, one might attempt to bias combinatorial chemistry efforts to produce a set of molecules, which contain drug like patterns such as the pyridine heterocyclic ring [21]. The study of the vibrational spectra of substituted pyridine mainly amino pyridine attracts the attention of many spectroscopists due to their wide application in pharmacology and agro-chemistry. Pyridine heterocycles are a repeated moiety in many large molecules with interesting photo physical, electrochemical, and catalytic applications [22–29]. They serve as good anesthetic agent and hence are used in the preparation of drugs for certain brain disease. These pharmaceutically acceptable results and the pre-drugs are used for the treatment (or) prevention of diabetic neuropathy [30, 31]. The vibrational studies of substituted pyridine have been the subject of several investigations [32–34]. More recently [35, 36], the FTIR and FT-Raman spectra of amino pyridine and amino picoline have been reported together with the vibrational assignments of the vibrational modes. Sundaraganesan et al. [37–39] reported the FTIR spectra of 2-amino-5-chloropyridine, 2-amino-5-iodopyridine and 4-N,N'-dimethylamino pyridine by HF and DFT calculations. Sundaraganesan et al. [40] studied the molecular structure and vibrational spectra of 2-amino-5-methyl pyridine and 2-amino-6-methyl pyridine by density functional methods. Most recently, Ramalingam et al. [41] investigated the vibrational spectra of the 2-amino pyridine by using DFT and HF methods. Literature survey reveals that to the best of our knowledge neither the complete X-ray crystallography, IR and NMR spectra studies on 2-amino-3-bromopyridine 4-methylbenzoic acid have been reported so far. The ab initio and DFT calculations have been performed to support the bond parameters, wavenumber assignments, and chemical shifts have also been studied.

## 2. Materials and method

### 2.1. General remarks

All chemicals are reagent grade and used as commercially purchased without further purification. FTIR spectra were recorded on a PerkinElmer 2000 Spectrum in the form of KBr pellets.  $^1\text{H}$ -NMR and  $^{13}\text{C}$ -NMR spectra were recorded at 500 MHz, in DMSO- $d_6$ , on Bruker 500 MHz Avance III spectrometer. The chemical shifts are reported in parts per million (ppm) downfield from internal tetramethylsilane (TMS) (chemical shift in  $\delta$  values). PXRD diffractogram at 25°C provided another piece of information for the identification and crystallinity of starting materials and co-crystal. PXRD diffractogram was collected by BRUKER D8 ADVANCE DIFFRACTOMETER. The source of PXRD was  $\text{CuK}\alpha$  (1.542 Å) and the diffractometer was operated at 40 kV and 30 mA. The X-ray was passed through a 1 mm slit and the signal a 1 mm slit, a nickel filter, and another 0.1 mm slit. The detector type was a scintillation counter. The scanning rate was set at 0.05° ranging from 5° to 45°. The quantity of sample used was around 20–30 mg.

### 2.2. Synthesis

Both of the starting materials 2-amino-3-bromopyridine and 4-methylbenzoic acid were obtained from Sigma–Aldrich chemical suppliers. Analytical grade solvent was used for preparation of the cocrystal. The 1:1 mixture of 2-amino-3-bromopyridine (86 mg, 1 mmol) and 4-methylbenzoic acid (68 mg, 1 mmol) was dissolved in 20 mL of methanol by heating magnetic stirrer hotplate for a few minutes. The resulting solution was allowed to cool slowly at room temperature and crystals of the title cocrystal (**1**) appeared after a few days.

**Table 1.** Crystal data and structure refinement parameters for the 1:1 cocrystal of (2A3BP) with (4MBA).

CCDC deposition No.	1014582
Chemical formula	C <sub>5</sub> H <sub>5</sub> BrN <sub>2</sub> ·C <sub>8</sub> H <sub>8</sub> O <sub>2</sub>
Formula mass	309.16
Temperature (K)	100
Wavelength (Å)	0.71073 Mo K $\alpha$
Crystal system	Monoclinic
Space group	P2 <sub>1</sub> /c
<i>a</i> (Å)	12.7904 (8)
<i>b</i> (Å)	6.7626 (4)
<i>c</i> (Å)	15.4479 (10)
$\alpha$ (°)	90
$\beta$ (°)	108.785 (3)
$\gamma$ (°)	90
<i>V</i> (Å <sup>3</sup> )	1265.01 (14)
<i>Z</i>	4
<i>D<sub>c</sub></i> (g cm <sup>−3</sup> )	1.623
<i>F</i> (000)	624
$\theta$ range (°)	2.8–29.8
Measured reflns	18457
Unique reflns	2890
Observed reflns ( <i>I</i> > 2 $\sigma$ ( <i>I</i> ))	2240
No. of parameters	176
<i>R</i> <sup>(a)</sup>	0.077
<i>wR</i> <sup>(b)</sup>	0.215
<i>GOF</i> <sup>(c)</sup>	1.20
Residual peaks (e·Å <sup>−3</sup> )	1.00, −2.17
( $\Delta/\sigma$ ) <sub>max</sub>	0.000

For 1,  $w = 1/[\sigma^2(F_o^2) + (0.087P)^2 + 6.4503P]$ , where  $P = (F_o^2 + 2F_c^2)/3$ ; [a]  $R = \Sigma ||F_o| - |F_c|| / \Sigma |F_o|$ , [b]  $R_w = \{w \Sigma (|F_o| - |F_c|)^2 / \Sigma w |F_o|^2\}^{1/2}$ , [c]  $GOF = \{\Sigma w (|F_o| - |F_c|)^2 / (n-p)\}^{1/2}$ , where *n* is the number of reflections and *p* the total number of parameters refined.

### 2.3. Crystallography

Single crystal suitable for X-ray analysis was performed on Bruker SMART APEXII CCD diffractometer using MoK $\alpha$  radiation ( $\lambda = 0.71073$  Å). Data Collection was performed by using the APEX2 software [42], whereas the cell refinement and data reduction were performed under the SAINT software [42]. The complete crystallographic data were collected at 100 (1) K using the Oxford Cryosystem Cobra low temperature attachment [43] and the crystallographic data are shown in Table 1. The crystal structure was solved by direct methods using the program SHELXTL [44] and refined by full-matrix least squares technique on  $F^2$  using anisotropic displacement parameters using SHELXTL [44] program. Absorption correction was applied to the final crystal data by using the SADABS software [42]. All geometrical calculations were carried out using the program PLATON [45]. The molecular graphics were drawn using SHELXTL [44] program. Anisotropic thermal factors were assigned to all non-hydrogen atoms. The O- and N-bound hydrogen atoms were located in a difference Fourier map. Atoms H1N2 and H2N2 were refined freely, while atom H1O1 was refined with a bond restraint O–H = 0.82 (1) Å [refined distances O1–H1O1 = 0.821(10) Å, N2–H1N2 = 0.90(10) Å and N2–H2N2 = 0.94(7) Å]. The remaining hydrogen atoms were positioned geometrically (C–H = 0.95–0.98 Å) and were refined using a riding model, with  $U_{iso}(H) = 1.2U_{eq}(C)$  or  $1.5U_{eq}(\text{methyl } C)$ . A rotating group model was applied to the methyl groups.

### 2.4. Computational details

The theoretical calculations were performed by the Hartree-Fock (HF) and Density Functional Theory (Becke's non-local three parameter exchange and the Lee, Young and Parr;

B3LYP) methods by the Gaussian 09 [46] program package in 6-311+G(d,p) basis set. The molecular geometries were optimized to standard convergence criteria and further used to calculate the vibrational wave numbers and isotropic chemical shifts. The calculated vibrational frequencies are corresponded to potential energy minima which no imaginary frequency was found. Due to neglect of the anharmonicity in the real system, the scaling factors of 0.9668 at B3LYP level and of 0.9059 at HF level [47] were used to suit the calculated vibrational wavenumbers with experimental data. The gauge-invariant atomic orbital (GIAO) method was used to calculate the  $^1\text{H}$  and  $^{13}\text{C}$  NMR chemical shifts in ppm relative to TMS as internal standard. The GIAO approach allows the computation of the absolute chemical shielding due to the electronic environment of the individual nuclei and this method is often more accurate than those calculated with other approaches for the same basis set [48]. Gauss View molecular visualization program have been used for animation of vibrational band assignments and preparation of the spectrum [49].

### 3. Results and discussion

#### 3.1. Description of molecular structure and crystal packing

Cocrystal **1** of the composition [(2A3BP)(4MBA)] was prepared by reacting equal mol of 2-amino-3-bromopyridine and 4-methylbenzoic acid in 1:1 ratio, which crystallizes as monoclinic colourless crystals in the centrosymmetric space group  $P2_1/c$ . The structure of **1** with the atom numbering scheme is shown in Fig. 1. A search in the Cambridge Structural Database (CSD, Version 5.35 of May 2014; Allen, 2002) [50] for organic compounds including only the elements C, H, O, N, and Br was conducted, and revealed 16 crystal structures containing both 2-aminobromopyridine and aromatic/aliphatic carboxylic acid, with such a supramolecular heterosynthon observed in all of them. In the structures with code of WIGWUG [51], DUSQAK [52], DUVCIH [53], KUSTEY [54], LADBOJ [55], LADBUP [55], MISMAC [56], PUKDOP [57], PUKJIP [58], SUYNUW [59], SUYXIU [60], SUYYAN [61], SUZBEV [62], and SUZZIX [63] the 2-aminobromopyridine is a cation forming salts, and in PUKDIJ [64] and DUSKUY [65] 2-aminobromopyridine is a neutral molecule forming a cocrystals. Table 2 shows a comparison between the experimental, calculated structural parameters with the similar 2-aminobromopyridine crystal structures (CSD refcodes: PUKDIJ [64], DUSKUY [65]).

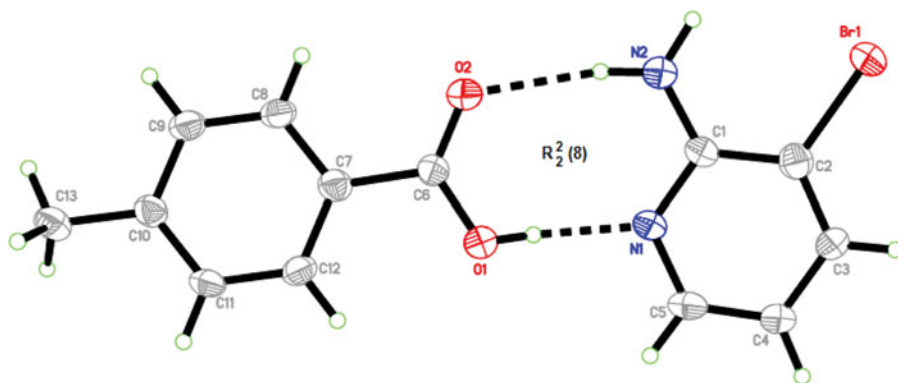


**Figure 1.** An ORTEP view of the title cocrystal showing the atom-numbering scheme. Displacement ellipsoids are drawn at the 50% probability level.

**Table 2.** Experimental and optimized geometrical parameters of the title cocrystal.

Parameters	Experimental	Calculated		PUKDIJ [64]	DUSKUY [65]
		HF 6-311+G(d,p)	DFT B3LYP 6-311+G(d,p)		
Bond lengths (Å)					
Br1—C2	1.880 (6)	1.89995	1.91760	1.887(2)	1.889(10)
O1—C6	1.302 (7)	1.31057	1.32783	1.317(2)	1.307(11)
O2—C6	1.240 (7)	1.19583	1.22496	1.225(2)	1.249(10)
N1—C5	1.348 (7)	1.32515	1.33863	1.355(3)	1.322(11)
N1—C1	1.357 (7)	1.32840	1.35079	1.349(3)	1.351(11)
N2—C1	1.356 (8)	1.34443	1.34819	1.339(3)	1.349(12)
C6—C7	1.497 (8)	1.48703	1.48809	1.493(3)	1.474(13)
C10—C13	1.498 (8)	1.50931	1.50837	—	—
Bond angles (°)					
C5—N1—C1	119.6 (5)	119.78799	119.99125	118.98(18)	119.3(8)
N2—C1—N1	117.0 (5)	117.45217	117.64388	118.04(19)	115.5(8)
N2—C1—C2	123.8 (5)	122.70177	123.19676	120.74(19)	124.6(8)
N1—C1—C2	119.2 (5)	119.83951	119.15935	121.21(19)	119.9(8)
C3—C2—Br1	120.8 (5)	119.75603	119.93824	120.10(16)	120.5(8)
C1—C2—Br1	118.9 (4)	120.54571	119.69552	120.26(16)	120.5(8)
N1—C5—C4	123.6 (5)	124.12096	123.66711	122.22(10)	123.1(9)
O2—C6—O1	123.9 (5)	122.78957	123.27376	123.04(18)	122.8(8)
O2—C6—C7	121.3 (5)	123.14075	122.64539	120.31(18)	122.3(8)
O1—C6—C7	114.8 (5)	114.06967	114.08083	116.65(16)	114.9(7)
C11—C10—C13	121.5 (5)	121.03805	120.93259	—	—
C9—C10—C13	120.0 (5)	120.49414	120.83205	—	—
Torsion angles (°)					
C5—N1—C1—N2	178.0 (5)	178.86529	179.97262	177.14(19)	179.8(8)
C5—N1—C1—C2	− 2.4 (9)	− 0.22872	0.00339	− 1.8(3)	− 0.6(13)
N2—C1—C2—C3	− 177.5 (6)	− 178.87891	− 179.97283	− 177.5(2)	177.5(9)
Br1—C2—C3—C4	179.2 (5)	179.97280	179.99660	178.02(16)	178.4(6)
O2—C6—C7—C12	− 175.1 (6)	179.90818	179.84195	− 166.0(19)	− 178.3(8)
O1—C6—C7—C12	5.2 (9)	− 0.11348	− 0.19614	13.7(3)	2.6(12)
O2—C6—C7—C8	4.1 (9)	0.07068	0.03166	12.0(3)	1.1(13)
O1—C6—C7—C8	− 175.7 (6)	− 179.95098	179.99357	− 168.26(2)	− 178.1(8)

In general, the experimental [(2A3BP)(4MBA)] bond length and bond angle values are comparable with the corresponding values obtained by similar crystal structures [64,65]. The non-hydrogen atoms of the 2-amino-3-bromopyridine molecule is essentially planar, with maximum deviation of 0.031 (6) Å for atom N2. The dihedral angle between the pyridine (N1/C1–C5) and benzene (C7–C12) rings is 4.2(3)°. The acid molecule is essentially planar, with a dihedral angle of 4.8(7)° between the benzene (C7–C12) ring and carboxylic (O1/O2/C6) group. This value is slightly similar with the observed 2-aminobromopyridine neutral molecule of cocrystals PUKDIJ [12.97(11)°] and DUSKUY [2.5(9)°]. The C–N–C bond angle in pyridine is known to be sensitive to protonation [66,67] and its cationic form a higher value than the corresponding neutral molecules. The C1–N1–C5 bond angles in pyridine ring in **1** is 119.6(5)°. This bond angle values of 118.98(18)° and 119.3(8)° are also observed in the cocrystals of PUKDIJ [64] and DUSKUY [65], respectively. This value is in good agreement with the C–N–C bond angle in the free aromatic nitrogen atom of pyridine ring encountered in 213 neutral 2-aminopyridines with an average value of 116(2)° [68]. In addition, the C–O distances for COOH [C6–O1 & C6–O2] group of the 4-methylbenzoic acid are 1.302(7) & 1.240(7) Å, respectively. Meanwhile, the similar range of bond length distances of 1.317(2) Å & 1.225(2) Å in PUKDIJ and 1.307(11) Å & 1.249(10) Å in DUSKUY are also observed. These values emphasize the fact that cocrystal **1** is formed only via a strong hydrogen bond between the proton-donor and proton-acceptor compounds; no proton transfer occurs. C–N–C bond angles in cocrystal containing a acid-pyridine hetero supramolecular



**Table 3.** Hydrogen bonding geometry for title cocrystal.

D—H...A	D—H (Å)	H...A (Å)	D...A (Å)	D—H...A (°)
O1—H1O1...N1	0.82 (9)	1.77 (9)	2.571 (7)	165 (8)
N2—H1N2...O2	0.90 (11)	2.10 (10)	2.976 (7)	167 (9)
N2—H2N2...O2 <sup>i</sup>	0.94 (8)	2.20 (8)	3.098 (7)	162 (6)
C9—H9A...Br1 <sup>ii</sup>	0.95	2.81	3.582 (7)	139
C13—H13C...Cg1 <sup>iii</sup>	0.98	2.87	3.813 (8)	163

Symmetry codes: (i)  $-x + 1, y + 1/2, -z + 1/2$ ; (ii)  $-x + 1, y - 3/2, -z + 1/2$ ; (iii)  $-x + 2, -y + 1, -z + 1$ .

synthon were investigated in some other studies and found to be in full agreement with what we report herein [69–75]. All the bond lengths and angles are in the normal ranges [76].

In cocrystal **1**, the 2A3BP molecules interact with the carboxylic group of the respective 4MBA molecules through N2—H1N2...O2 and O1—H1O1...N1 hydrogen bonds to form a cyclic hydrogen-bonded ring motif,  $R_2^2(8)$  [77]. The motif has been observed in the crystal structure of all 2-aminopyridine carboxylic acid cocrystals [65,78] and it is one of the top five ring motifs among the 24 most frequently observed hydrogen-bonded cyclic bimolecular motifs (supramolecular synthons) [79]. These motifs are further interconnected by supramolecular heterosynthons  $N_{(am)} \cdots O_{(COOH)}$  hydrogen bonds (Table 3) formed between the N—H of amine groups ( $N \cdots O$ : 3.098 (7) Å; symmetry code:  $-x + 1, y + 1/2, -z + 1/2$ ) and carboxyl oxygen (O2), forming a helical chain running along the *b* axis (Fig. 2a). Further, these supramolecular chains are interconnected to neighboring chain through weak C—H...Br hydrogen bonds ( $C \cdots Br$  = 3.582 (7) Å; symmetry code:  $-x + 1, y - 3/2, -z + 1/2$ ) involving bromine atom (Br1) and one of the hydrogen atom (H9A) from C9 carbon atom, forming one-dimensional supramolecular chain along the *b* axis (Fig. 2b). Adjacently arranged heterosynthons units in two different planes are attacked through  $\pi$ – $\pi$  interactions between an 4-methylbenzoic acid molecule and a pyridine base rings with Cg–Cg distance 3.805(4) Å, interplanar distance 3.437(2) Å and slip angle (The angle between the centroid vector and the normal to the plane) of 25.12°. The crystal structures are further stabilized by weak C—H... $\pi$  zig-zag chain interactions along *b*-axis, involving the C7–C12 (centroid Cg1; symmetry code:  $-x + 2, -y + 1, -z + 1$ ; Fig. 2c) ring, to form a 2-D layer network (Fig. 2d). A similar type of C—H... $\pi$  interaction has been investigated on the basis of the structural data determined by X-ray diffraction [80–82].

### 3.2. Optimized structures

The labeling of atoms in 2-amino-3-bromopyridine 4-methylbenzoic acid is given in Fig. 3. The optimized geometrical parameters (bond length and bond angles) of the title compound were obtained using by HF and B3LYP with the 6-311+G(d,p) basis sets. Some selected geometric parameters experimentally obtained and theoretically calculated are listed in Table 2.

As can be seen from Table 2, most of the optimized bond lengths are slightly longer than the experimental values and the bond angles are slightly different from the experimental values. We note that the experimental results are for the solid phase and the theoretical calculations are for the gas phase. The C–O bond lengths of the COOH group are slightly different in X-ray [ $C6-O1$  = 1.302 (7) Å and  $C6-O2$  = 1.240(7) Å], while these bond lengths have been calculated at 1.31057 Å and 1.19583 Å for HF and 1.32783 Å and 1.22496 Å for B3LYP method using 6-311+G(d,p) basis set, respectively. The C–O bond lengths in the carboxylic acid group are intermediate between single  $Csp^2-O$  (1.308–1.320 Å) and double  $Csp^2 = O$  bond values (1.214–1.224 Å) [76] which clearly distinguishes the neutral molecule of the acid. In the

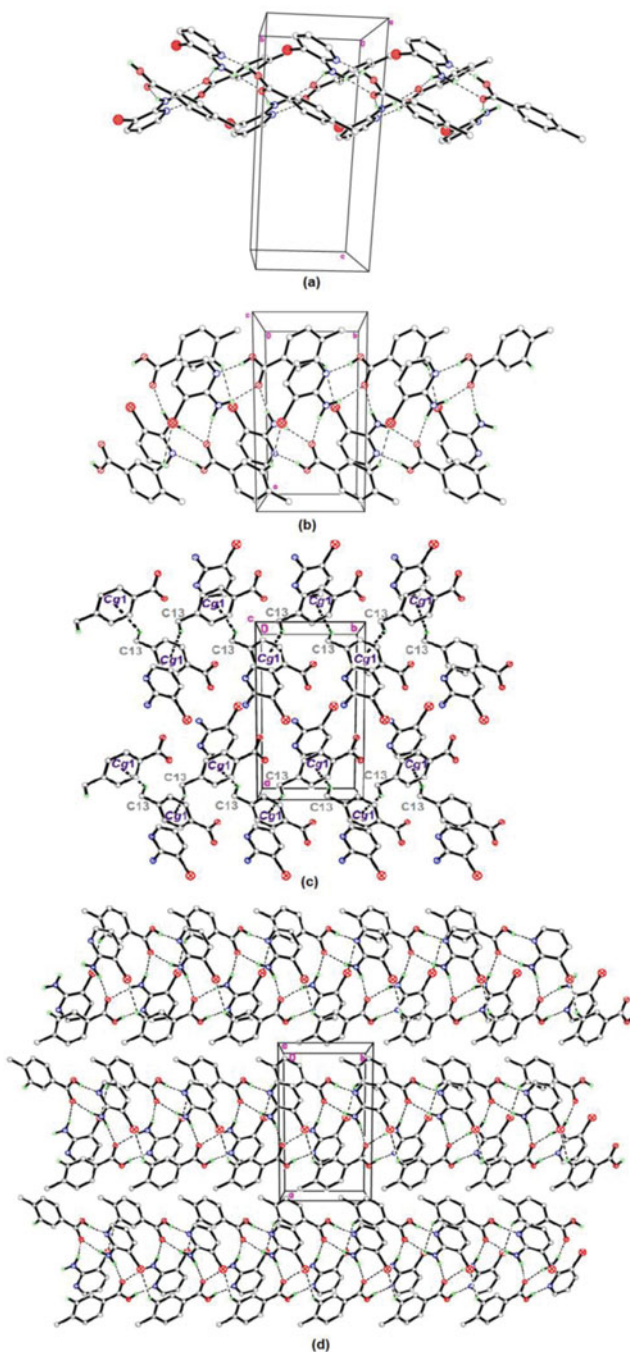


**Figure 2.** Hydrogen bonding interactions in title cocrystal: (a). supramolecular heterosynths to form helical chain; (b). supramolecular one-dimensional chain formed via C—H...Br interactions; (c). C—H... $\pi$  zig-zag chain interactions (c). The crystal packing of the compound connected into a two-dimensional network. Dashed lines show the intermolecular hydrogen bonds. H atoms not involved in hydrogen bonding are omitted for clarity



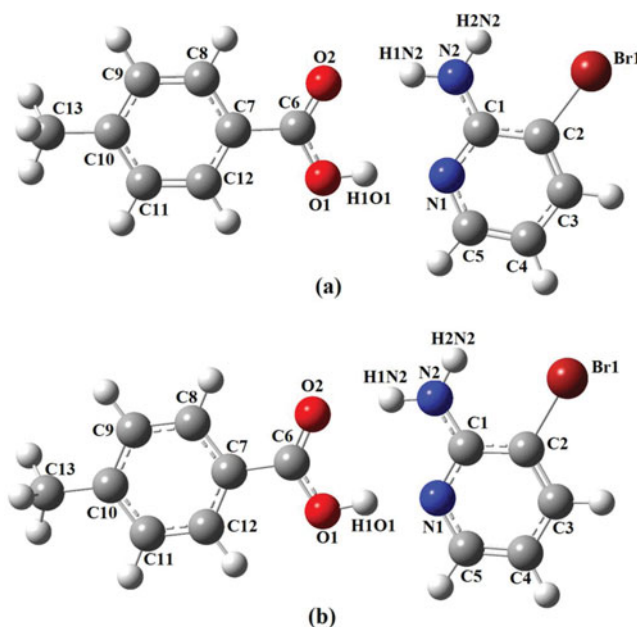


**Figure 3.** The optimized structure at the (a) HF/6311+G(d,p) and (b) B3LYP/6311+G(d,p) level of theory of the 1:1 cocrystal of 2-amino-3-bromopyridine with 4-methylbenzoic acid.

2A3BP ring, the bond angles of C1–N1–C5 was obtained to be  $119.6(5)^\circ$  in X-ray while these bond angles have been calculated at  $119.78799^\circ$  and  $119.99125^\circ$  with HF and B3LYP method using 6-311+G(d,p) basis set, respectively.

The X-ray structure of the title compound is compared with its optimized counterparts (see Fig. 3) and slight conformational discrepancies are observed between them. The most notable discrepancies exist in the orientation of the carboxylic group of the 4-methylbenzoic acid molecule. The orientation of the carboxylic group from the experimental data is defined by torsion angles of O1–C6–C7–C12 [ $5.2(9)^\circ$ ], O2–C6–C7–C12 [ $-175.1(6)^\circ$ ], O1–C6–C7–C8 [ $-175.7(6)^\circ$ ], and O2–C6–C7–C8 [ $4.1(9)^\circ$ ]. These torsion angles have been calculated at  $-0.11348^\circ$ ,  $179.90818^\circ$ ,  $-179.95098^\circ$ , and  $0.07068^\circ$  for HF and  $-0.19614^\circ$ ,  $179.84195^\circ$ ,  $179.99357^\circ$ , and  $0.03166^\circ$  for B3LYP method using 6-311+G(d,p) basis set, respectively. The angle differences for about  $4\text{--}5^\circ$  are due to the effect of intermolecular interactions observed in the crystal packing.

### 3.3. Vibrational assignments

The harmonic vibrational frequencies were calculated for (2A3BP) (4MBA) at HF and B3LYP levels using the triple split valence basis set along with diffuse and polarization function, 6-311+G(d,p). All the experimental and theoretical vibrational frequencies for the synthesized compound (2A3BP) (4MBA), along with corresponding vibrational assignments and intensities are given in Table 4. The bands observed in the measured region  $4000\text{--}400\text{ cm}^{-1}$  arise from the internal vibrations of the amino groups, pyridine ring, and 4-methylbenzoic acid. The calculated (HF and DFT) and experimental vibrational frequencies are comparable to each other where the correlation values of 0.996 for HF and 0.998 for DFT are obtained. According to these results, there is a good correlation between the theoretical and experimental vibrational frequencies. The correlation graph is shown in Fig. 4.

**Table 4.** Comparison of the observed and calculated vibrational spectra of the title cocrystal.

Experiment (cm <sup>-1</sup> )	Calculated IR (km mol <sup>-1</sup> ) HF 6-311+Gdp		DFT B3LYP 6-311+G(dp)		Assignments <sup>(a)</sup>
	Unscaled	Scaled	Unscaled	Scaled	
3418.56	3946.69	3575.31	3691.85	3576.66	$\nu_{as}NH_2$
3316.22	3759.35	3405.60	3391.05	3285.25	$\nu_sNH_2, \nu_sOH,$
3194.35	3372.87	3055.48	3210.65	3110.48	$\nu_sCH$
	3372.70	3055.33	3206.90	3106.84	$\nu_sCH$
	3367.76	3050.85	3198.91	3099.10	$\nu_sCH$
	3352.02	3036.59	3192.60	3092.99	$\nu_sCH$
	3326.08	3013.10	3162.99	3064.30	$\nu_{as}CH$
	3325.06	3012.17	3162.96	3064.28	$\nu_{as}CH$
	3322.49	3009.84	3161.88	3063.23	$\nu_sCH$
2975.80	3246.69	2941.18	3104.65	3007.78	$\nu_sCH_3$
	3222.45	2919.22	3077.27	2981.26	$\nu_{as}CH$
2922.20	3167.25	2869.21	3022.34	2928.04	$\nu_sCH_3$
1681.47	1926.35	1745.08	1723.37	1669.60	$\rho OH, \nu C=O, \delta NH_2$
1632.39	1820.68	1649.35	1678.94	1626.56	$\delta NH_2$
1608.88	1798.72	1629.46	1650.47	1598.98	$\nu_sCC, \delta CH$
1574.94	1778.68	1611.31	1633.36	1582.40	$\delta NH_2, \nu_sCC, \nu_sCN, \rho CH$
1540.72	1750.03	1585.35	1608.25	1558.07	$\nu CC, \rho CH_3, \rho CH, \rho OH$
1508.87	1736.96	1573.51	1576.06	1526.89	$\nu_sCN, \nu_sCC, \rho CH, \rho OH, \nu CO$
	1673.81	1516.30	1542.49	1494.36	$\rho CH, \rho OH, \nu CC$
	1611.60	1459.95	1525.76	1478.16	$\nu_sCN, \rho OH, \nu CC, \rho CH$
1471.92	1609.61	1458.15	1492.64	1446.07	$\delta CH_3, \rho CH$
	1606.13	1454.99	1489.72	1443.24	$\delta CH_3$
1445.33	1571.23	1423.38	1488.03	1441.60	$\rho CH, \rho OH, \nu CC, \nu CN, \delta CH_3,$
1405.33	1603.51	1452.62	1474.82	1428.81	$\rho CH, \rho OH, \nu CC, \nu CN, \delta CH_3$
1382.98	1544.86	1399.49	1435.14	1390.36	$\nu CC, \rho CH, \rho CH_3, \rho OH$
	1537.51	1392.83	1413.85	1369.74	$\omega CH_3$
1369.04	1458.47	1321.23	1361.35	1318.88	$\nu CC, \nu CN, \rho CH, \rho NH_2, \rho OH$
1317.40	1446.41	1310.30	1341.99	1300.12	$\nu CC, \nu CO, \rho CH, \rho OH, \rho CH_3$
	1315.42	1191.64	1333.40	1291.80	$\rho CH, \nu CC, \rho CH_3$
1290.19	1407.98	1275.49	1318.36	1277.23	$\nu CC, \nu CN, \nu CO, \rho NH_2, \rho CH, \rho OH$
1176.17	1280.04	1159.59	1291.16	1250.88	$\nu CC, \nu CN, \rho CH, \rho NH_2$
1142.20	1289.61	1168.26	1202.51	1164.99	$\rho CH$
1127.88	1238.74	1122.17	1160.55	1124.34	$\rho CH, \rho NH_2, \nu CC, \nu CN$
1114.00	1225.55	1110.23	1144.21	1108.51	$\rho CH, \nu CC, \nu CO$
	1184.13	1072.70	1134.40	1099.01	$\rho CH, \rho CH_3, \nu CC, \nu CO$
1066.92	1168.61	1058.64	1094.33	1060.19	$\rho CH, \rho NH_2, \nu CC$
	1134.27	1027.54	1075.73	1042.17	$\rho NH_2, \rho CH, \nu CC$
1017.88	1159.34	1050.25	1060.58	1027.49	$\rho CH, \rho CH_3$
	969.70	878.45	1038.21	1005.82	$\rho OH$
	1108.97	1004.62	1036.94	1004.59	$\nu CC, \delta CH$
	1106.12	1002.03	1025.47	993.48	$\nu CC, \nu CN, \rho NH_2$
	1082.63	980.75	1006.60	975.19	$\rho CH_3, \rho CH$
	1114.06	1009.23	999.64	968.45	$tCH, \rho OH$
	1085.92	983.73	987.95	957.13	$tCH, \rho CH_3$
	1103.08	999.28	973.56	943.18	$tCH$
	944.51	855.63	883.30	855.74	$\nu CC, \nu CN$
830.84	947.98	858.78	861.65	834.77	$\omega CH, \omega CH_3$
	891.62	807.72	838.76	812.59	$\nu CC, \nu CO$
	864.18	782.86	781.87	757.48	$\omega CH$
758.27	941.57	852.97	774.06	749.91	$\omega CH, \nu CC$
	815.01	738.32	766.52	742.60	$\nu CC, \nu CO$
749.16	842.15	762.90	761.32	737.57	$\nu CC, \nu CN$
	676.62	612.95	731.89	709.06	$\omega NH_2$
688.89	761.82	690.13	705.54	683.53	$\omega CH, \omega CH_3, \omega NH_2$
639.05	727.65	659.18	686.03	664.63	$\nu CC, \nu CN$
	695.44	630.00	652.30	631.95	$\nu CC$
583.84	653.12	591.66	616.42	597.19	$\nu CC, \nu CO$
	628.05	568.95	587.07	568.75	$\nu CC, \nu CN$
550.60	603.11	546.36	559.92	542.45	$\omega CH$
511.99	556.95	504.54	529.62	513.10	$\rho NH_2, \rho CH, \rho CC$

(Continued)

Table 4. Continued

Experiment (cm <sup>-1</sup> )	Calculated IR (km mol <sup>-1</sup> ) HF 6-311+Gdp		DFT B3LYP 6-311+G(dp)		Assignments <sup>(a)</sup>
	Unscaled	Scaled	Unscaled	Scaled	
483.59	516.23	467.65	487.22	472.02	$\rho\text{NH}_2$
	527.27	477.65	484.23	469.12	$\omega\text{CC}$
425.43	480.96	435.70	438.69	425.00	$\omega\text{CH}$
	457.88	414.79	418.64	405.58	$\tau\text{CH}$
	387.41	350.95	369.71	358.18	$\nu\text{CC}$
	375.27	339.96	354.24	343.19	$\rho\text{CH}$ , $\rho\text{CH}_3$
	320.54	290.38	325.31	315.16	$\omega\text{NH}_2$
	332.02	300.78	303.52	294.05	$\nu\text{CBr}$ , $\nu\text{CC}$
	303.35	274.80	280.56	271.81	$\omega\text{CH}$
	250.39	226.83	238.61	231.17	$\rho\text{CBr}$
	261.58	236.97	238.08	230.65	$\omega\text{NH}$ , $\omega\text{CC}$
	237.76	215.39	235.25	227.91	$\rho\text{CO}$ , $\rho\text{CH}_3$
	152.80	138.42	142.87	138.41	Skeletal vibration
	124.64	112.91	113.81	110.26	Skeletal vibration
	94.10	85.25	104.09	100.84	Skeletal vibration
	79.84	72.33	87.63	84.90	Skeletal vibration
	78.75	71.34	74.44	72.12	Skeletal vibration
	41.20	37.32	47.98	46.48	Skeletal vibration
	51.24	46.42	47.47	45.99	Skeletal vibration
	24.02	21.76	29.55	28.63	$\rho\text{CH}_3$
	19.51	17.67	22.15	21.46	Skeletal vibration
	15.34	13.90	16.90	16.37	Skeletal vibration

<sup>a</sup> Vibrational assignment:  $\nu$ , stretching;  $\nu_{as}$ , asymmetric stretching;  $\nu_s$ , symmetric stretching;  $\delta$ , scissoring;  $\omega$ , wagging;  $\rho$ , rocking;  $t$ , twisting.

The hydroxyl vibrations are likely to be the most sensitive to the environment, so they show pronounced shifts in the spectra of the hydrogen-bonded species. Generally the O—H stretching vibrations are seen in the region of 3600–3400 cm<sup>-1</sup> [83]. The O—H stretching vibration is observed at 3316 cm<sup>-1</sup>, while it is calculated at 3405 cm<sup>-1</sup> for HF and 3285 cm<sup>-1</sup> for DFT, respectively. While the in-plane O—H bending mode was calculated at 1321 cm<sup>-1</sup> for HF method and 1318 cm<sup>-1</sup> for with B3LYP method, it was observed experimentally at 1317 cm<sup>-1</sup>.

The amino group has two types of stretching vibrations. One being asymmetric and other is symmetric. Usually, the N—H stretching vibrations occur in the region 3500–3300 cm<sup>-1</sup>. The FT-IR spectrum of the title aminopyridine compound contains intense broad bands in the range of the  $\nu\text{N—H}$  vibrations. The two bands at 3418 and 3316 cm<sup>-1</sup> correspond to the stretching vibrations of N—H bonds. These bands have been calculated at 3575 and 3405 cm<sup>-1</sup> with HF method and 3576 and 3285 cm<sup>-1</sup> with B3LYP method using 6-311+G(d,p) basis set. Bellamy [84] and Mancy et al. [85] suggested that the N-H<sub>2</sub> scissoring mode lies in the region of 1529–1650 cm<sup>-1</sup>. We assigned the band at 1632 cm<sup>-1</sup> due to the N-H<sub>2</sub> scissoring which appeared at 1649 for HF and 1626 cm<sup>-1</sup> for DFT, respectively, in the theoretical spectra. The N-H<sub>2</sub> rocking and wagging modes recorded at 1127 and 688 cm<sup>-1</sup>, respectively, are comparable with theoretical results of 1122 and 690 cm<sup>-1</sup> with HF and 1124 and 683 cm<sup>-1</sup> with B3LYP method using 6-311+G(d,p) basis set.

The band observed in the 1700–1800 cm<sup>-1</sup> region due to the C = O stretching vibration is one of the characteristic features of the carboxylic group. The band appears at 1681 cm<sup>-1</sup> is assigned as C = O stretching vibration in FTIR spectrum. Meanwhile, the calculated C = O frequencies are found at 1745 cm<sup>-1</sup> from HF method and 1669 cm<sup>-1</sup> with B3LYP

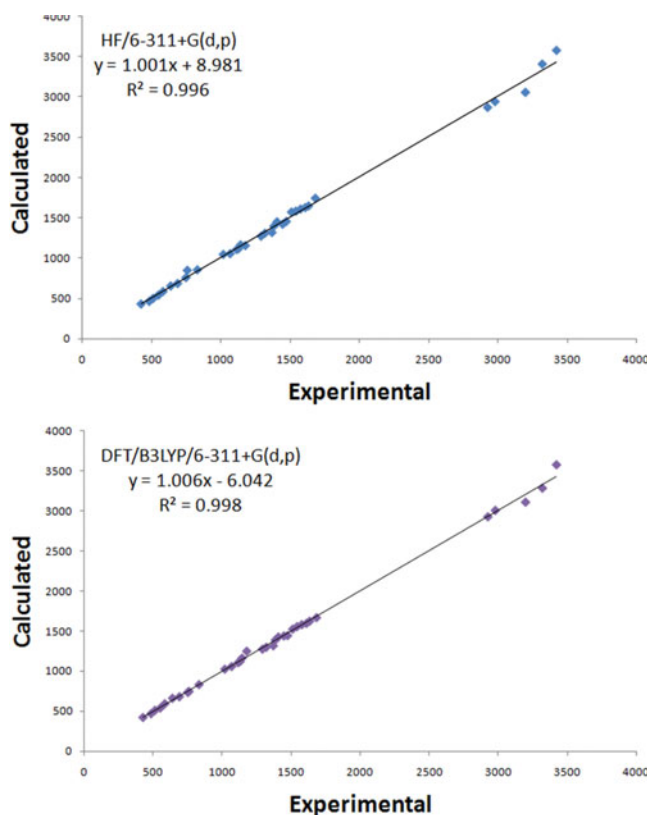


**Figure 4.** The linear correlation graphics between calculated and experimental vibrational frequencies of cocrystal 1.

method. Additionally, if a neutral O—H ... N hydrogen bond was formed between the components, then a broad stretch near  $1900\text{ cm}^{-1}$  was viewed as an evidence for cocrystal formation [86,87].

The absorption bands at  $3194$  and  $3012\text{ cm}^{-1}$  correspond to the aromatic C—H stretching vibrations of the title cocrystal that have been calculated at  $3055\text{--}3009\text{ cm}^{-1}$  for HF and  $3110\text{--}3063\text{ cm}^{-1}$  for DFT, respectively. The stretching vibration of the aromatic C—CH<sub>3</sub> group of the title cocrystal was observed at  $2922\text{ cm}^{-1}$  which are in accordance with theoretical results of  $2869\text{ cm}^{-1}$  for HF and  $2928\text{ cm}^{-1}$  with B3LYP method using 6-311+G(d,p) basis set. The C—C stretching mode of the aromatic ring of the compound was appeared  $1540\text{ cm}^{-1}$  while the C—N stretching vibration was observed at  $1508\text{ cm}^{-1}$ .

Mooney [88,89] assigned the vibrations of the C—X group (X = F, Cl, Br, and I) in the wavenumber range of  $1129\text{--}480\text{ cm}^{-1}$ . The heavier mass of bromine obviously makes the C—Br stretching mode to appear at longer wavelength region ( $200\text{--}480\text{ cm}^{-1}$ ) as reported by Varsanyi [90]. The assignments of the C—Br stretching and deformation vibrations have been made by comparison with similar molecules, such as, *p*-bromophenol and the halogen substituted benzene derivatives [90]. The C—Br stretching vibration is assigned to the strong mode  $300\text{ cm}^{-1}$  for HF and  $294\text{ cm}^{-1}$  for DFT in the infrared spectra.

The other vibrational bands of 2-amino-3-bromopyridine 4-methylbenzoic acid are shown in Table 4. It can be stated that the experimental and theoretical vibrational bands of 2-amino-3-bromopyridine 4-methylbenzoic acid are in a comparable to each other.

### 3.4. NMR spectra analysis

The  $^1\text{H}$  and  $^{13}\text{C}$  NMR spectra of cocrystal were carried out in DMSO- $d_6$  at room temperature using TMS as internal standard. The optimized structure of (2A3BP)(4MBA) is used to calculate the NMR spectra at the HF and DFT (B3LYP) methods with 6-311+G(d,p) level using the GIAO method. The results of the calculated values shifted to higher values of chemical shift and further corrected with the TMS isotropic chemical shift values. The theoretical  $^1\text{H}$  and  $^{13}\text{C}$  NMR chemical shifts of (2A3BP)(4MBA) have been compared with the experimental data as shown in Table 5. As can be seen from the table, the experimental chemical shift values are comparable with the theoretical values.

In the  $^1\text{H}$  NMR spectra of the compound, the  $\text{NH}_2$  protons in the 2-aminopyridine appear at 7.94 ppm, while these signals are observed computationally at 7.88 (H1N2), 4.57 (H2N2) ppm with HF and 9.76 (H1N2), 4.96 (H2N2) ppm with B3LYP method using 6-311+G(d,p) basis set. The differences between the experimental and calculated values are due to the formation of motif (heterodimer) by the  $\text{N2}\cdots\text{H1N2}\cdots\text{O2}$  hydrogen bond observed in the

**Table 5.** Experimental and theoretical  $^1\text{H}$  and  $^{13}\text{C}$  isotropic chemical shifts (ppm) for the title cocrystal.

Chemical Shift (ppm) <sup>a</sup>	Experimental	Calculated HF 6-311+G (d,p) <sup>b</sup> & B3LYP 6-311+G (d,p) <sup>c</sup>									
		Cocrystal		Homodimers				Monomers			
				(2A3BP) (2A3BP)		(4MBA)(4MBA)		2A3BP		4MBA	
		HF	B3LYP	HF	B3LYP	HF	B3LYP	HF	B3LYP	HF	B3LYP
$^1\text{H}$ NMR											
O1-H1O1	12.8081	11.878	14.9955			11.0474	13.8614			5.4655	5.7221
N2-H1N2	7.9462	7.8813	9.7675	7.8081	9.9249			4.3624	4.5665		
N2-H2N2		4.5735	4.9618	4.486	4.9674			4.1293	4.5284		
Aromatic proton	6.18–7.8	8.864,	8.4999,	8.3863	8.0093						
		8.6968	8.3858	8.1667	7.6140	8.875	8.5369	8.4317	8.2015	8.7913	8.4389
		8.4086	8.0343,	6.5395	6.4535	8.7183	8.4267	8.1235	7.6246	8.511	8.2739
		8.1814	7.6584			7.5853	7.4703	6.6011	6.5799	7.578	7.4935
		7.5897	7.4377,			7.4987	7.4684			7.4468	7.4403
		7.4882	7.4347								
		6.4927	6.4726								
Methyl group	2.35–2.51	2.7198	2.7198								
		2.5082	2.5082			2.7261	2.7518			2.7004	2.6819
		2.279	2.279			2.4829	2.7507			2.5052	2.4039
						2.3107	2.3841			2.245	2.2836
$^{13}\text{C}$ NMR											
C6	167.29	171.911	177.601			173.779	179.354			167.401	171.588
C1	156.24	168.532	163.514	168.49	163.63			166.843	162.586		
C5	146.90	158.526	151.373	158.783	152.05			159.331	154.522		
C3	142.95	157.242	147.538	156.268	146.708			155.24	146.298		
C10	140.10	157.340	151.373			155.214	152.474			154.852	152.027
C8	129.28	142.272	138.063			142.541	138.249			142.421	138.539
C12	129.05	141.583	137.071			142.031	137.398			141.182	137.004
C9	128.05	132.389	134.335			132.251	134.393			132.66	134.756
C11	113.52	131.462	133.868			131.554	134.026			131.477	134.225
C7		130.999	134.883			129.954	133.368			129.094	132.237
C2	103.11	113.476	126.567	113.723	126.12			113.968	126.051		
C4		110.487	116.108	111.533	116.329			113.656	118.892		
C13	21.06	21.734	23.9071			21.7037	23.9062			21.5979	23.7853

<sup>a</sup>The atoms numbering are referred to the X-ray molecular diagram in Fig. 1.

<sup>b</sup>The isotropic chemical shift with respect to TMS in HF 6-311+G (d,p) are 3.2.4495 ppm for  $^1\text{H}$  NMR and 195.8342 ppm for  $^{13}\text{C}$  NMR.

<sup>c</sup>The isotropic chemical shift with respect to TMS in B3LYP 6-311+G (d,p) are 31.9844 ppm for  $^1\text{H}$  NMR and 184.0085 ppm for  $^{13}\text{C}$  NMR.

molecular structure. The same range of chemical shift values are found in the homodimers (2A3BP.2A3BP and 4MBA.4MBA), showing the presence of intermolecular N—H...N hydrogen bonds between N2-H1N2 bond with the pyridine group and the formation of intermolecular O—H...O hydrogen bonds between O1-H1O1 bond with the carboxylic group, respectively. In monomers,  $\delta$  values are found to be lower compared to the  $\delta$  values of heterodimer and homodimers where values of amino group and carboxylic group are 4.5665 ppm and 5.7221 ppm with B3LYP method using 6-311+G(d,p) basis set. The other chemical shifts values of monomers, homodimers, and cocrystal are shown in Table 5. In the experimental  $^1\text{H}$  NMR spectrum, the signal at 12.80 ppm (11.878 ppm in HF and 14.99 in DFT spectrum) confirms the presence of carboxylic proton (COOH) of 4-methylbenzoic acid moiety. The signals at 6.18–7.85 ppm range are typical for hydrogen atoms attached to aromatic ring. The presence of the methyl group in 4MBA gave single peaks at  $\delta$  values of 2.50 ppm and the values of the calculated chemical shift of methyl group were also in same range of 2.7198–2.279 ppm for HF and 2.7425–2.3426 ppm for B3LYP method using 6-311+G(d,p) basis set.

The  $^{13}\text{C}$  NMR spectrum given in Table 5, clearly shows the cocrystal of (2A3BP)(4MBA). And 4-methylbenzoic acid gives a single signal at 167.29 ppm for COOH (C6) carbon atom. This signals has been calculated at 171.911 ppm for HF method and 177.601 ppm with B3LYP method using 6-311+G(d,p) basis set, respectively. These values also in good agreement with the previous reported structure [91]. The C atoms (C13) of methyl groups are observed at 21.06 ppm. These peaks theoretically calculated at 21.734 and 23.9071 ppm with HF and B3LYP method using 6-311+G(d,p) basis set. As can be seen from Table 5, the theoretical  $^1\text{H}$  and  $^{13}\text{C}$  NMR chemical shift values for the title compound are generally comparable to the experimental  $^1\text{H}$  and  $^{13}\text{C}$  NMR chemical shift data.

### 3.5. Powder XRD of cocrystal

Powder XRD is a useful method for fast identification of the new phases [92,93]. A different PXRD pattern for the cocrystal from those of the individual components confirms the formation of a new phase. The PXRD patterns of 2-amino-3-bromopyridine and 4-methylbenzoic acid cocrystal has been depicted in Fig. 5. The PXRD pattern of 2-amino-3-bromopyridine shows some characteristic peaks at  $7.5^\circ$ ,  $14.1^\circ$ ,  $15.2^\circ$ ,  $17.2^\circ$ ,  $22.7^\circ$ ,  $24.7^\circ$ ,  $24.7^\circ$ ,  $26.2^\circ$ ,  $29.1^\circ$ ,  $30.8^\circ$ ,  $31.7^\circ$ ,  $34.8^\circ$ ,  $36.7^\circ$ ,  $38.7^\circ$ ,  $40.2^\circ$ , and  $42.9^\circ$  ( $2\theta$ ) while the PXRD pattern of 4-methylbenzoic acid shows characteristic peaks at  $12.4^\circ$ ,  $13.7^\circ$ ,  $14.5^\circ$ ,  $15.4^\circ$ ,  $17.2^\circ$ ,  $22.6^\circ$ ,  $24.9^\circ$ ,  $26.5^\circ$ ,  $27.8^\circ$ ,  $29.4^\circ$ ,  $30.6^\circ$ ,  $31.3^\circ$ ,  $32.4^\circ$ ,  $33.0^\circ$ ,  $35.0^\circ$ ,  $36.4^\circ$ ,  $39.9^\circ$ , and  $40.8^\circ$  ( $2\theta$ ). The PXRD pattern of [(2A3BP)(4MBA)] cocrystal 1 shows appearance of new peaks at  $6.9^\circ$ ,  $15.3^\circ$ ,  $17.4^\circ$ ,  $20.2^\circ$ ,  $23.3^\circ$ ,  $24.7^\circ$ , and  $26.7^\circ$  ( $2\theta$ ). Besides this, characteristics peaks of (2A3BP) at ( $14.1^\circ$ ,  $22.7^\circ$ , and  $30.8^\circ$ ) and of (4MBA) at ( $12.4^\circ$  and  $32.4^\circ$ ) have disappeared in the PXRD pattern of [(2A3BP)(4MBA)]. From the above results, it is clear that there is transformation in the crystalline lattices of 2-amino-3-bromopyridine and 4-methylbenzoic acid and new phases have been formed. In addition, the powder diffraction patterns generated with the single-crystal data of compound 1 using Mercury [94] show small difference with the experimental PXRD spectra measured using the D5000 powder diffractometer. This is particularly due to the fact that the single crystal X-ray diffraction was taken at low temperature (100 K) compared to room temperature in the powder X-ray diffraction.

### 3.6. Prediction of cocrystals/salts by pKa values

The relevance of pKa can act as a predictor either cocrystals or salts for carboxylic acids and pyridines [95].  $\Delta$  pKa of carboxylic acid vs.  $N_{\text{arom}}$  moieties can be used to predict whether



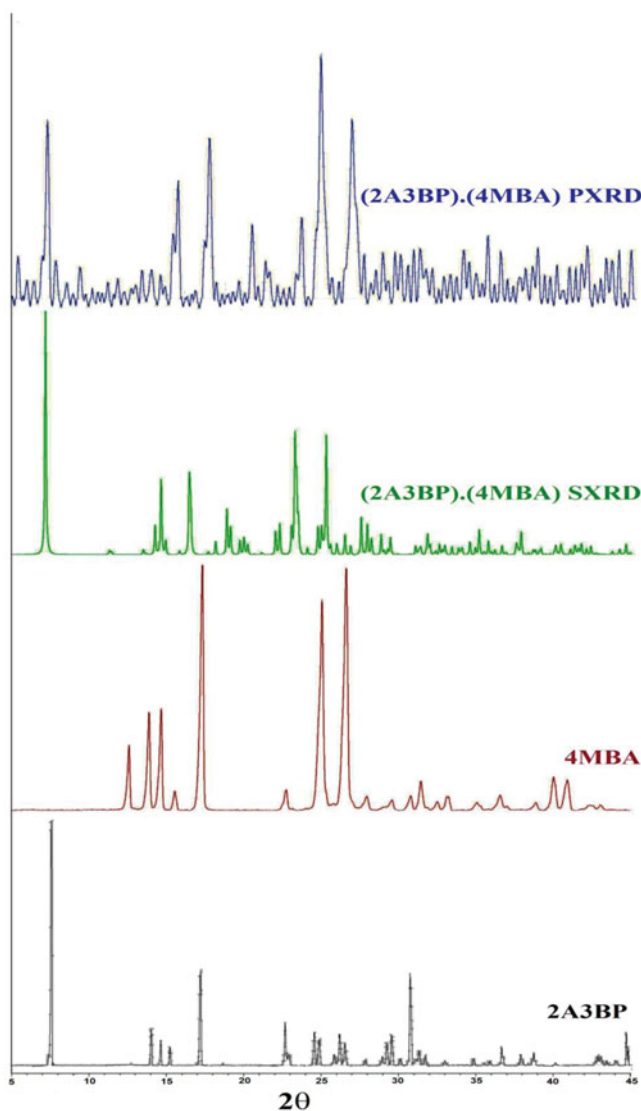


**Figure 5.** Comparison of PXRD patterns of the cocrystal and the individual components under various conditions.

or not proton transfer will occur [ $\Delta pK_a = pK_a(2A3BP) - pK_a(4MBA)$ ]. Generally, a sufficiently large  $\Delta pK_a$  value (i.e. greater than 3) should result in a salt [96]. With smaller  $\Delta pK_a$  values, a cocrystal can be expected, but this parameter seems inappropriate for accurately predicting salt or cocrystal formation in the solid state when  $0 < \Delta pK_a < 3$  [97, 98]. In this study, the  $pK_a$  values for 2-amino-3-bromopyridine and 4-methylbenzoic acid are 5.22 and 4.26, respectively, while  $\Delta pK_a$  values for this acid–base complex are 0.96 and lead to the formation of cocrystal.

## Conclusions

In this study, we have synthesized a [(2A3BP)(4MBA)] cocrystal and characterized by PXRD, spectroscopy (FT-IR,  $^1H$  NMR, and  $^{13}C$  NMR) and structural determination (single-crystal

X-ray diffraction) techniques. To support the solid state structure, the geometric parameters, vibrational frequencies and  $^1\text{H}$  NMR and  $^{13}\text{C}$  NMR chemical shifts of the title cocrystal have been calculated using the HF and B3LYP method with 6-311+G(d,p) basis sets and compared with the experimental findings. The experimental geometric parameters, vibrational frequencies and chemical shift values are in a comparable agreement with the experimental findings. The discrepancies between the experimental and theoretical geometric parameters, IR frequencies, chemical shift values are mainly due to the hydrogen bonding interactions since all the hydrogen bound to the nitrogen and oxygen atoms are involved in hydrogen bonding in the crystal structure. PXRD indicated the formation of the cocrystal by solid-state grinding.

## Supplementary Materials

This data (CCDC:1014582) can be obtained free of charge at [www.ccdc.cam.ac.uk/conts/retrieving.html/](http://www.ccdc.cam.ac.uk/conts/retrieving.html/) or from the Cambridge Crystallographic Data Centre (CCDC), 12 Union Road, Cambridge CB2 IEZ, UK; fax: +44(0) 1223-336033; e-mail: [deposit@ccdc.cam.ac.uk](mailto:deposit@ccdc.cam.ac.uk)

## Acknowledgments

The authors thank the Malaysian Government and Universiti Sains Malaysia (USM) for the research facilities and USM Short Term Grant, No. 304/PFIZIK/6312078 to conduct this work. KT thanks the Academy of Sciences for the Developing World and USM for the TWAS–USM fellowship. NCK thanks the Ministry of Education Malaysia for the MyBrain15 Myphd scholarships. The authors thank to Mohd Sukeri Mohd Yusof from Universiti Malaysia Terengganu for the Gaussian09 software used in the theoretical calculation.

## References

- [1] Panunto, T. W., Lipkowska, Z. U., Johnson, R., & Etter, M. C. (1987). *J. Am. Chem. Soc.*, 109, 7786.
- [2] Shan, N., & Zaworotko, M. J. (2008). *Drug Discovery Today*, 13(3), 440.
- [3] Etter, M. C. (1991). *J. Phys. Chem.*, 95, 4601.
- [4] Etter, M. C., Lipkowska, Z. U., Mohammad Zia-Ebrahimi, S., & Panunto, T. W. (1990). *J. Am. Chem. Soc.*, 112, 8415.
- [5] Etter, M. C., Reutzel, S. M., & Choo, C. G. (1993). *J. Am. Chem. Soc.*, 115, 4411.
- [6] Wöhler, F. (1844). *Untersuchungen über das Chinon, Annalen.*, 51, 153.
- [7] Ling, A. R., & Baker, J. L. (1893). *J. Chem. Soc.*, 63, 1314.
- [8] Desiraju, G. R. (2003). *Cryst. Eng. Commun.*, 5, 466.
- [9] Lapidus, S. H., Stephens, P. W., Arora, K. K., Shattock, T. R., & Zaworotko, M. J. (2010). *Cryst. Growth Des.*, 10(10), 4630.
- [10] Dunitz, J. D. (2003). *Cryst. Eng. Commun.* 5, 506.
- [11] Thomas, L. H., Florenceb, A. J., & Wilson, C. C. (2009). *New J. Chem.*, 33, 2486.
- [12] Hathwar, V. R., Pal, R., & Guru Row, T. N. (2010). *Cryst. Growth Des.*, 10(8), 3306.
- [13] Bond, A. D., Jones, W. (2002). In: *Supramolecular Organization and Materials Design*, Jones, W., Rao, C. N. R., Eds., Cambridge University Press: Cambridge, pp. 391–443.
- [14] Arenas-Garcia, J. I., Herrera-Ruiz, D., Mondragon-Vasquez, K., Morales-Rojas, H., & Hopfl, H. (2010). *Cryst. Growth Des.*, 10(8), 3732.
- [15] Atwood, J. L., Davies, J. E. D., MacNicol, D. D., & Vogtle, F. (1996). *Comprehensive Supramolecular Chemistry*, Pergamon: Oxford.
- [16] Cheney, M. L., Weyna, D. R., Shan, N., Hanna, M., Wojtas, L., & Zaworotko, M. J. (2010). *Cryst. Growth Des.*, 10(10), 4401.
- [17] Sarfraz, A., Simo, A., Fenger, R., Christen, W., Rademann, K., Panne, U., & Emmerling, F. (2012). *Cryst. Growth Des.*, 12, 583.
- [18] Bolton, O., Simke, L. R., Pagoria, P. F., & Matzger, A. J. (2012). *Cryst. Growth Des.*, 12, 4311.

- [19] Bailey Walsh, R. D., Bradner, M. W., Fleischman, S., Morales, L. A., Moulton, B., Hornedo, N. R., & Zaworotko, M. J. (2003). *Chem. Commun.*, 186.
- [20] Pozharskii, A. F., Soldatenkov, A. T., & Katritzky, A. R. (1997). *Heterocycles in Life and Society*, John Wiley and Sons: UK.
- [21] Bemis, G. W., & Murcko, M. A. (1996). *J. Med. Chem.*, 39, 2887.
- [22] Zucchi, F., Trabanelli, G., & Gonzalez, N. A. (1995). *J. ACH Models Chem.*, 132, 4579.
- [23] Khan, B. T., Khan, S. R. A., & Annapoorna, K. (1995). *Ind. J. Chem. Soc.*, 34, 11878.
- [24] Lizarraga, M. E., Navarro, R., & Urriolabeitia, E. P. (1997). *J. Org. Metal. Chem.*, 542, 51.
- [25] Georgopoulou, A. S., Ulvenlund, S., Mingos, D. M. P., Baxter, I., & Williams, D. J. (1999). *J. Chem. Soc.*, 4, 547.
- [26] Liaw, W., Lee, N., Chen, C., Lee, C., Lee, G., & Peng, S. (2000). *J. Am. Chem. Soc.*, 122, 488.
- [27] Trotter, P. J., & White, P. A. (1978). *J. Appl. Spectrosc.*, 32, 323.
- [28] Rajpure, K. Y., & Bhosale, C. H. (2000). *J. Mater. Chem. Phys.*, 64, 70.
- [29] Licht, S. (1995). *J. Solar Energy Mater. Solar Cells.*, 38, 305.
- [30] Altenburger, J. M., Lassalle, G. Y., Matrougui, M., Galtier, D., Jetha, J. C., Bocskei, Z., Berry, C. N., Lunven, C., Lorrain, J., Herault, J. P., Schaeffer, P., Connor, S. E. O., & Herbert, J. M. (2004). *Bioorg. Med. Chem.*, 12, 1713.
- [31] Kandasamy, M. & Velraj, G. (2012). *Spectrochimica Acta Part A*, 91, 206–216.
- [32] Topaci, A., & Bayari, S. (2001). *Spectrochim. Acta A*, 57, 1385.
- [33] Medhi, R. N., Borman, R., Medhi, K. C., & Jois, S. S. (2000). *Spectrochim. Acta A*, 56, 1523.
- [34] Tocon, I. L., Wooley, M. S., Otero, J. C., & Marcos, J. I. (1998). *J. Mol. Struct.*, 470, 241.
- [35] Jose, S. P., & Mohan, S. (2006). *Spectrochim. Acta A*, 64, 240.
- [36] Mostafa, A., & Bazzi, H. S. (2009). *Spectrochim. Acta A*, 74, 180.
- [37] Sundaraganesan, N., Illakiamani, S., Anand, B., Saleem, H., & Joshua, B. D. (2006). *Spectrochim. Acta A*, 64, 586.
- [38] Sundaraganesan, N., Meganathan, C., Anand, B., Joshua, B. D., & Lapouge, C. (2007). *Spectrochim. Acta A*, 67, 830.
- [39] Sundaraganesan, N., Kalaichelvan, S., Meganathan, C., Joshua, B. D., & Cornard, J. P. (2008). *Spectrochim. Acta A*, 71, 898.
- [40] Sundaraganesan, N., Meganathan, C., & Kurt, M. (2008). *J. Mol. Struct.*, 891, 284.
- [41] Ramalingam, S., Periandy, S., & Mohan, S. (2010). *Spectrochim. Acta A*, 77, 73.
- [42] Bruker (2009). *SADABS, APEX2 and SAINT*. Bruker AXS Inc: Madison.
- [43] Cosier, J., & Glazer, A. M. (1986). *J. Appl. Cryst.*, 19, 105.
- [44] Sheldrick, G. M. (2008). *Acta Cryst.*, A64, 112.
- [45] Spek, A. L. (2009). *Acta Cryst.*, D65, 148.
- [46] Frisch, M. J. et al. (2009). *Gaussian 09, Revision A.1*, Gaussian, Inc.: Wallingford, CT.
- [47] Merrick, J. P., Moran, D., & Radom, L. (2007). *J. Phys. Chem. A*, 111, 11683.
- [48] Atiş, M., Karipchi, F., Sariboğa, B., Taş, M., & Çelik, H. (2012). *Spectrochim. Acta A*, 98, 290.
- [49] Dennington, R., Keith, T., & Millam, J. (2009). *GaussView*, Version 5, Semichem Inc.: Shawnee Mission KS.
- [50] Allen, F. H. (2002). *Acta Cryst.*, B58, 380.
- [51] Thanigaimani, K., Khalib, N. C., Arshad, S., & Razak, I. A. (2013). *Acta Cryst.*, E69, o537.
- [52] Hemamalini, M., & Fun, H.-K. (2010). *Acta Cryst.*, E66, o1964.
- [53] Quah, C. K., Hemamalini, M., & Fun, H.-K. (2010). *Acta Cryst.*, E66, o2164.
- [54] Hemamalini, M., & Fun, H.-K. (2010). *Acta Cryst.*, E66, o775.
- [55] Aakeroy, C. B., Rajbanshi, A., Li, Z. J., & Desper, J. (2010). *Cryst. Eng. Commun.*, 12, 4231.
- [56] Vaday, S., & Foxman, B. M. (1999). *Cryst. Eng.*, 2, 145.
- [57] Hemamalini, M., & Fun, H.-K. (2010). *Acta Cryst.*, E66, o664.
- [58] Hemamalini, M., & Fun, H.-K. (2010). *Acta Cryst.*, E66, o689.
- [59] Hemamalini, M., & Fun, H.-K. (2010). *Acta Cryst.*, E66, o2200.
- [60] Hemamalini, M., & Fun, H.-K. (2010). *Acta Cryst.*, E66, o2246.
- [61] Quah, C. K., Hemamalini, M., & Fun, H.-K. (2010). *Acta Cryst.*, E66, o2252.
- [62] Quah, C. K., Hemamalini, M., & Fun, H.-K. (2010). *Acta Cryst.*, E66, o2269.
- [63] Hemamalini, M., & Fun, H.-K. (2010). *Acta Cryst.*, E66, o2408.
- [64] Hemamalini, M., & Fun, H.-K. (2010). *Acta Cryst.*, E66, o663.
- [65] Quah, C. K., Hemamalini, M., & Fun, H.-K. (2010). *Acta Cryst.*, E66, o1935.

- [66] Boenigk, D., & Mootz, J. (1998). *J. Am. Chem. Soc.*, 110, 2135.
- [67] Cowan, J. A., Howard, J. A. K., McIntyre, G. J., Lo, S. M.-F., & Williams, I. D. (2003). *Acta Cryst.*, B59, 794.
- [68] Alshahateet, S. F. (2010). *Mol. Cryst. Liq. Cryst.*, 533, 152.
- [69] Vishweshwar, P., Nangia, A., & Lynch, V. M. (2002). *J. Org. Chem.*, 67, 556.
- [70] Walsh, R. D. B. et al. (2003). *Chem. Commun.*, 2, 186.
- [71] Steiner, T. (2001). *Acta Cryst.*, B57, 103.
- [72] Vishweshwar, P., Nangia, A., & Lynch, V. M. (2003). *Cryst Growth Des.*, 3(5), 783.
- [73] Etter, M. C., & Adsmond, D. A. (1990). *J. Chem. Soc., Chem. Commun.*, 8, 589.
- [74] Aakeroy, C. B., Beatty, A. M., & Helfrich, B. A. (2002). *J. Am. Chem. Soc.*, 124(48), 14425.
- [75] Bhogala, B. R., Vishweshwar, P., & Nangia, A. (2002). *Cryst Growth Des.*, 2(5), 325.
- [76] Allen, F. H., Kennard, O., Watson, D. G., Brammer, L., Orpen, A. G., & Taylor, R. (1987). *J. Chem. Soc. Perkin. Trans.*, 2, S1–19.
- [77] Bernstein, J., Davis, R. E., Shimoni, L., & Chang, N.-L. (1995). *Angew. Chem. Int. Ed. Engl.*, 34, 1555.
- [78] Hemamalini, M., & Fun, H.-K. (2010). *Acta Cryst.*, E66, o578.
- [79] Allen, F. H., Raithby, P. R., Shields, G. P., & Taylor, R. (1998). *Chem. Commun.*, 1043.
- [80] Thanigaimani, K., Arshad, S., Razak, I. A., Makesvaran, D., & Balasubramani, K. (2013). *Acta Cryst.*, E69, o970.
- [81] Khalib, N. C., Thanigaimani, K., Arshad, S., & Razak, I. A. (2014). *J. Chem. Crystallogr.*, Doi: 10.1007/s10870-014-0550-2
- [82] Quah, C. K., Hemamalini, M., & Fun, H.-K. (2010). *Acta Cryst.*, E66, o1933–o1934.
- [83] Silverstein, R. M., & Webster, F. X. (1998). *Spectroscopic Identification of Organic Compound*, 6th ed., John Wiley & Sons: New York.
- [84] Bellamy, L. J. (1980). *The Infrared spectra of Complex Molecules*, vol. 2. Chapman and Hall: London.
- [85] Mancy, S., Peticoles, W. L., & Toblas, R. S. (1979). *Spectrochim. Acta A.*, 35, 315.
- [86] Child, S. L., Patrick Stahly, G., & Park, A. (2007). *Mol. Pharmaceut.*, 4(3), 323.
- [87] Aakeroy, C. B., Desper, J., & Fasulo, M. E. (2006). *Cyst. Eng. Commun.*, 8(8), 586.
- [88] Mooney, E. F. (1964). *Spectrochim. Acta*, 20, 1021.
- [89] Monney, E. F. (1963). *Spectrochim. Acta*, 19, 877.
- [90] Varsanyi, G. (1974). *Assignments of Vibrational Spectra of 700 Benzene Derivatives*, Wiley: New York.
- [91] Hosseini, H. E. et al. (2011). *Spectrochim. Acta A*, 78, 1392.
- [92] Trask, A. V., van de Streek, J., Samuel Motherwell, W. D., & Jones, W. (2005). *Cryst. Growth Des.*, 5(6), 2233.
- [93] Trask, A. V., Samuel Motherwell, W. D., & Jones, W. (2004). *Chem. Commun.*, 890–891.
- [94] Macrae, C. F. et al. (2006). *J. Appl. Cryst.*, 39, 453.
- [95] Weyna, D. R., Shattock, T. R., Vishweshwar, P., & Zaworotko, M. J. (2009). *Cryst. Growth Des.*, 9(2), 1106.
- [96] Bhogala, B. R., Basavoju, S., & Nangia, A. (2005). *Cryst. Eng. Commun.*, 7, 551.
- [97] Portalone, G., & Colapietro, M. (2009). *J. Chem. Cryst.*, 39, 193.
- [98] Portalone, G. (2011). *Chem. Cent. J.*, 5, 51.